


 Cite this: *RSC Adv.*, 2026, 16, 16249

# First example of an electropolymerizable heptazine bearing oligothiophene arms: a new way to produce well-defined heptazine-containing polymers

 Irena Kulszewicz-Bajer,<sup>\*a</sup> Pierre Audebert,<sup>id \*bc</sup> Hemender Chand<sup>c</sup> and Marzena Banasiewicz<sup>d</sup>

 Received 16th December 2025  
 Accepted 18th February 2026

DOI: 10.1039/d5ra09746k

[rsc.li/rsc-advances](https://rsc.li/rsc-advances)

We prepared the first example of a heptazine molecule bearing three arms, each of them functionalized with a terminal thiophene. This novel molecule is strongly fluorescent, benefiting from the energy transfer between the strongly absorbing heptazine and strongly emitting benzothiadiazole-thiophene segments. This new molecule should enable multiple types of graftings by leveraging the various reactivities of the terminal thiophene moiety.

## Introduction

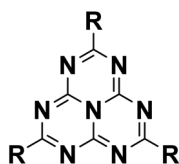
Heptazines (Scheme 1) constitute a remarkable category of aromatic, nitrogen-rich, fused tricyclic heterocycles.<sup>1–3</sup> However, in contrast to their parent tetrazines,<sup>4</sup> they display benzene-type aromaticity and related fluorescence. Because of their high nitrogen content and large bandgap, they present a high reduction potential, especially in their excited states. Their electron deficiency actually places them between triazines<sup>5</sup> and tetrazines,<sup>4</sup> the two other most widespread classes of related aromatic nitrogen-rich heterocycles. In regards with the previously studied nitrogen containing heterocycles, heptazines have yet attracted surprisingly much less attention. Nevertheless, we recently showed that some heptazines are photocatalysts<sup>6</sup> because of their highly oxidizing excited states and can trigger irreversible photoinduced electron transfer. We have already

outlined the importance of having in our hands well-characterized molecular heptazines, instead of heptazine-containing polymers.<sup>1</sup>

However, grafting in a controlled way, well characterized heptazine rings on a solid and produce a well-defined solid phase covered with heptazines, and presenting the properties of the grafted heptazines, still remains a desirable goal yet not attained outside a few examples of COFs,<sup>7–9</sup> MOFs,<sup>10,11</sup> and columnar liquid crystals.<sup>12</sup> Addressable heptazines grafted on, or contained in a solid phase would indeed be especially interesting for applications in photocatalysis, and also electrochromism (smart windows). In particular, no examples of conjugated polymers including heptazines are known yet to date. Indeed, graphitic carbon nitrides,<sup>13–15</sup> which are by far the most commonly studied solids containing heptazine rings,<sup>3</sup> although better and better produced and characterized, still present many defects.

We hypothesize that coupling a heptazine with a classical electropolymerisable moiety could lead to a well-defined, electroactive, and conducting polymer, featuring active heptazines inside in a porous but covalent network, as we have previously demonstrated with tetrazines.<sup>16</sup>

The first step in this straightforward synthesis strategy was to functionalize a triaminoheptazine with thiophenes. To this end, we prepared the oligomer represented in Fig. 1, which presents a heptazine core substituted with non-conjugated thiophene-benzothiadiazole side-chains.



Scheme 1 Generic structure of heptazines.

<sup>a</sup>Faculty of Chemistry, Warsaw University of Technology, Noakowskiego 3, 00-664 Warsaw, Poland. E-mail: [ikulsz@ch.pw.edu.pl](mailto:ikulsz@ch.pw.edu.pl)
<sup>b</sup>Universite Paris-Saclay, ENS Paris-Saclay, CNRS, PPSM, 4, Av. Des Sciences, 91110 Gifs. Yvette, France. E-mail: [pierre.audebert@ens-paris-saclay.fr](mailto:pierre.audebert@ens-paris-saclay.fr)
<sup>c</sup>XLIM, UMR CNRS, 7252 Av. Albert Thomas, 87060 Limoges Cedex, France

<sup>d</sup>Institute of Physics, Polish Academy of Sciences, Al. Lotnikow 32/44, 02-668, Warsaw, Poland

## Results and discussion

### Syntheses

Some of us have already demonstrated how easy it was to introduce amino substituents by substituting pyrazoles, onto



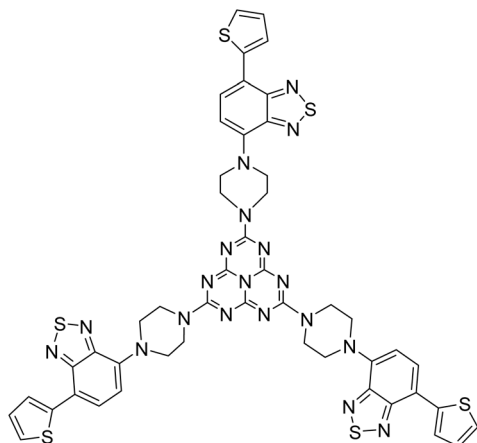


Fig. 1 Structure of dyad 1.

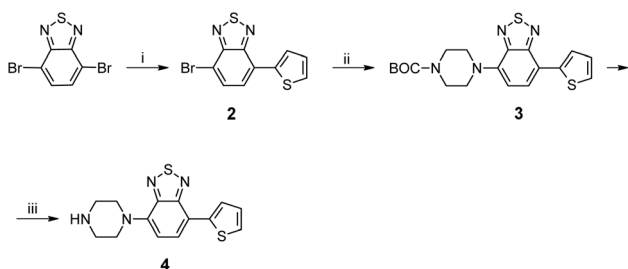
tris(diethylpyrazolyl)heptazine (TDPH). In order to polymerize without hopefully too many problems, it was attractive to choose a polymerizable thiophenic branch, substituted with a secondary amine (to avoid tautomeric effects after substitution on the heptazine), and so we chose to prepare benzothiadiazole,<sup>17</sup> bearing a polymerizable thienyl group on one side, and a piperazinyl on the other side, thus leaving a reactive NH group to be grafted on the TDPH, forming a tertiary amine after the substitution.

The synthetic route to the thiophenic branch is represented in Scheme 2.

Grafting on the TDPH was accomplished by nucleophilic substitution at ambient temperature under mild conditions similar to those employed in our previous study.<sup>1</sup> The amines can be readily grafted by nucleophilic substitution on the TDPH heptazine, which occurs nicely despite the high molecular weight of the substituted branch.

### Spectroscopy

The UV-visible spectrum of monomer 1 (Fig. S8) exhibits the spectral responses of both heptazine (280 and 300 nm) and the non-conjugated thienobenzothiadiazole branches (300 and 460 nm). The lowest energy band can be attributed to ICT between thiophene and benzothiadiazole units, as observed previously.<sup>19</sup>



Scheme 2 Synthetic route to the studied derivatives of benzothiadiazole: (i) 2-(tributylstannyl)thiophene, PdCl<sub>2</sub>(PPh<sub>3</sub>)<sub>2</sub>, THF, 85 °C; (ii) *tert*-butyl piperazine-1-carboxylate, sodium *tert*-butoxide Na(*t*-BuO), Pd(OAc)<sub>2</sub>, *t*-Bu<sub>3</sub>P, toluene, 110 °C and; (iii) TFA, CH<sub>2</sub>Cl<sub>2</sub>, K<sub>2</sub>CO<sub>3</sub>.

The PL spectrum of monomer 1 in toluene exhibited a broad (FWHM 150 nm) peak at 682 nm (Fig. S9), with no indication of any vibrational structure. This band was bathochromically shifted as compared to those recorded for thiophene-BTD<sup>17</sup> or amine-BTD<sup>20</sup> derivatives, indicating the electron-donating influence of the piperazine unit. The absorption spectrum of monomer 1 corresponds to the superposition of the absorption bands of the building blocks; *i.e.* heptazine and thienobenzothiadiazole moieties. However, the fluorescence spectrum of heptazine 1 reflects the excitation of the thienobenzothiadiazole-piperazine segments. This band (682 nm) is bathochromically shifted as compared to the PL spectra recorded for other benzothiadiazole derivatives. The large Stokes shift (222 nm) reflected the occurrence of ICT effects. The UV-visible spectrum of the branch features analogous bands, apart from the heptazines, which are absent.

### Electrochemistry

Since the ability of thiophenes to electropolymerize has long been known, the main goal of our approach was to prepare a conducting polymer containing heptazines using polymerizable thiophene branches (Fig. 2). Actually, the polymerization occurs nicely, as in similar cases, with the easy accumulative synthesis of an electroactive polymer (Fig. 3).

While the first reduction wave can be attributed to the benzothiadiazole cores, the second wave, close to the electrolyte limit, can be attributed to the triaminoheptazine system, by comparing the redox potential and the shape of the wave with the electrochemical response of the already studied tris(piperazine) heptazine.<sup>4,6</sup> The oxidation section of the CV is slightly more complicated, but the first oxidation peak can be attributed to the benzothiadiazole (BZT) branch, which should polymerize. The origin of the second oxidation step is unclear but probably corresponds to a second oxidation process on the same BZT branches, likely occurring after the coupling process. The shoulders on the main peaks can be attributed to small potential changes on neighboring branches on the same molecule, after the first local electron transfer on the first branch.

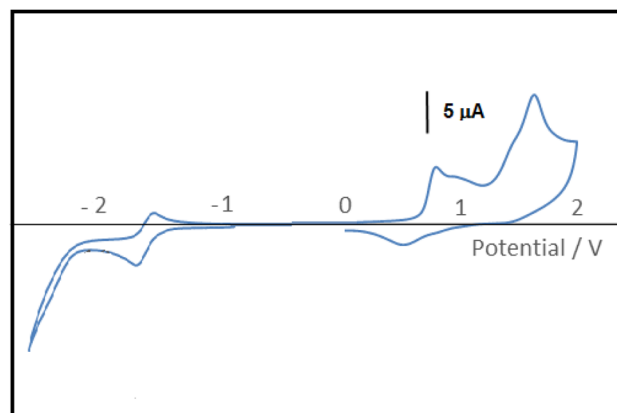


Fig. 2 CV of 1 in DCM/TBAFP (concentration ca.  $5 \times 10^{-4}$  M, Ref Ag/10<sup>-2</sup> M Ag<sup>+</sup> electrode). Oxidation and reduction CV plots are gathered from two separate experiments.



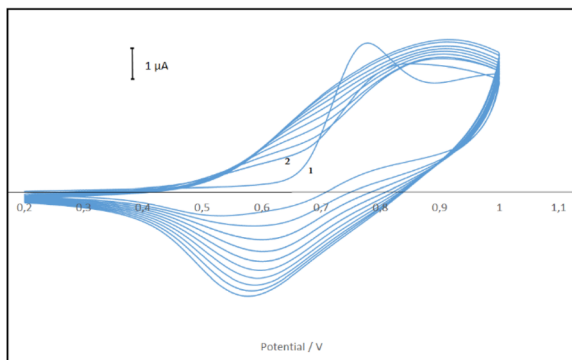


Fig. 3 Accumulative electrodeposition of poly(1) upon electrochemical oxidation (carbon electrode, DCM/TBAFP with concentration of about  $5 \times 10^{-4}$  M).

This result is corroborated by the fact that both electron transfers in the oxidation step have been found to be irreversible (up to  $5 \text{ V s}^{-1}$ ); moreover, repetitive CV cycling up to 1 V shows the appearance of a well-defined electroactive polymer that is accumulated regularly at the surface of the electrode (Fig. 3). It is not clear which part of the branch (the amine or the thiophene ring) is oxidized at the lowest potential, but anyhow, the induced positive charge density on the thienyl moieties, even in the case where the amine would be oxidized in first place, yet allows to trigger the polymerization reaction.

After its electrodeposition, the film can be cycled in a pure electrolyte without monomer, and shows the classical response of a polythiophene at a potential very close to the one of the monomer, the donating effect of the amines being otherwise compensated by the electron-withdrawing character of the benzothiadiazole units.

For comparison, we prepared an analogous branch to the one attached to the heptazine, with the slight modification of replacing the NH group of the terminal piperazine with an oxygen (molecule 5), to avoid complications due to the possible oxidation of the secondary amine, which could have possibly triggered complications with the observation of the thiophene oxidation. The synthesis of the branch alone occurs similarly to the one to be substituted on the TDPH (see SI Section and Scheme S3) and the UV spectrum of 5 (Fig. S10) recalls the one of compound 1, since the response of the heteroaryl branches is dominant over the heptazine one. Actually, the electrochemistry of the branch is also very similar to that of 1, displaying very similar oxidation potentials as expected, producing an electroactive dimer that precipitates on the electrode (Fig. S6). At negative potentials, the reduction of the thiophene-benzothiadiazole core occurs reversibly (Fig. S7), again at potentials close to that of compound 1, but slightly less negative, probably owing to the absence of the heptazine core.

Also, we have briefly examined the porosity of the polymer films, which is very small, since the films have been found to be compact at the molecular scale, as often the case with poly(heterocycles) like polypyrroles<sup>18</sup> or polythiophenes. Although BET experiments were not possible, we checked out, using electrochemistry, (Fig. S11 and 12) the film was completely non-

porous at the scale of the anthraquinone molecule, since no signal at all related to the anthraquinone reduction is observable on the electrode covered with poly(1) film. This demonstrates that the pores, if any, are indeed smaller than the anthraquinone molecule, while a clear classical reversible CV of anthraquinone on the same Pt electrode, non-covered with poly(1), can be observed (Fig. S13) (note: anthraquinone has been chosen since it is electroactive in the negative potentials region where the polymer is insulating; in the region where the polymer is conducting, of course no conclusion on the matter can be drawn, since the conducting polymer layer can drive electrons throughout).

## Conclusion

In this work, we demonstrated for the first time that heptazines could be linked to electropolymerizable units. Although aminoheptazines are not the most interesting units for photocatalytic applications, heptazine can be considered a nano (GCN) unit, and this provides a way to coat various substrates with GCN precursors. It should be noted that such polymeric networks do not disturb the possibility of bonding water molecules to the peripheral nitrogen atoms of heptazine, which is crucial for the photocatalytic activity of this unit. In conclusion, stable and relatively compact films containing well-defined heptazine units with precisely defined and identical chemical structures are obtained.

## Conflicts of interest

There are no conflicts to declare.

## Data availability

The data supporting this article have been included as part of the supplementary information (SI). Supplementary information is available. See DOI: <https://doi.org/10.1039/d5ra09746k>.

## Acknowledgements

This work was partially supported by the National Science Centre, Poland (NCN, Grant Opus No. 2022/45/B/ST5/02120), and partially funded by the LabEx Sigma-lim ANR-10-LBX-0074, Laboratory of Excellence, launched by the French Ministry of Higher Education and Research (<https://www.unilim.fr/labex-sigma-lim>) between the Institutes IRCER (<https://www.ircer.fr>) and XLIM (<https://www.xlim.fr>). The authors also wish to thank Dr Clémence Allain (PPSM laboratory) and Pr Adam Pron (WUT, Faculty of Chemistry) for their important contributions to this study.

## References

- 1 P. Audebert, E. Kroke, C. Posern and S.-H. Lee, *Chem. Rev.*, 2021, **121**, 2515–2544.
- 2 A. Schwarzer, T. Saplinova and E. Kroke, *Coord. Chem. Rev.*, 2013, **257**, 2032–2062.



- 3 S. Kumar, N. Sharma and K. Kailasam, *J. Mater. Chem. A*, 2018, **6**, 21719–21728.
- 4 G. Clavier and P. Audebert, *Chem. Rev.*, 2010, **110**, 3299–3314.
- 5 A. R. Katritzky, C. A. Ramsden, J. A. Joule and V. V. Zhdankin, *Handbook of Heterocyclic Chemistry*, Elsevier, 2010.
- 6 T. Le, L. Galmiche, G. Masson, C. Allain and P. Audebert, *Chem. Commun.*, 2020, **56**, 10742–10745.
- 7 D. Chen, W. Chen, Y. Wu, L. Wang, X. Wu, H. Xu and L. Chen, *Angew. Chem., Int. Ed.*, 2023, **62**, e202217479.
- 8 Q.-Q. Dang, Y.-F. Zhan, X.-M. Wang and X.-M. Zhang, *ACS Appl. Mater. Interfaces*, 2015, **7**, 28452–28458.
- 9 K. Kailasam, S. Johannes, B. Hakan, Z. Guigang, B. Siegfried, W. Xinchun and T. Arne, *Macromol. Rapid Commun.*, 2013, **34**, 1008–1013.
- 10 R. Luebke, L. J. Weselinski, Y. Belmabkhout, Z. Chen, L. Wojtas and M. Eddaoudi, *Cryst. Growth Des.*, 2014, **14**, 414–418.
- 11 K. Liu, B. Li, Y. Li, X. Li, F. Yang, G. Zeng, Y. Peng, Z. Zhang, G. Li, Z. Shi, S. Feng and D. Song, *Chem. Commun.*, 2014, **50**, 5031–5033.
- 12 I. Bala, H. Singh, V. R. Battula, S. P. Gupta, J. De, S. Kumar, K. Kailasam and S. K. Pal, *Chem.–Eur. J.*, 2017, **23**, 14718–14722.
- 13 C. C. Chen, D. L. Tsai, H. T. Liu and J. J. Wu, *ACS Sustainable Chem. Eng.*, 2023, **11**, 6435–6444.
- 14 V. R. Battula, S. Kumar, D. K. Chauhan, S. Samanta and K. Kailasam, *Appl. Catal., B*, 2019, **244**, 313–319.
- 15 W. Zhang, C. Xu, T. Kobayashi, Y. Zhong, Z. Guo, H. Zhan, M. Pruski and W. Huang, *Chem.–Eur. J.*, 2020, **26**, 7358–7364.
- 16 P. Audebert and C. Allain, in *Progress in Heterocyclic Chemistry*, ed. G. W. Gribble and J. A. Joule, Elsevier, 2018, vol. 30, pp. 399–426.
- 17 R. Gańczarczyk, R. Rybakiewicz-Sekita, M. Gryszel, J. Drapała, M. Zagórska and E. D. Głowacki, *Adv. Mater. Interfaces*, 2023, **10**, 2300270.
- 18 P. Audebert and G. Bidan, *J. Electroanal. Chem. Interfacial Electrochem.*, 1985, **190**, 129–139.
- 19 P. Ledwon, N. Thomson, E. Angioni, N. J. Findlay and P. J. Skabara, *RSC Adv.*, 2015, **5**, 77303–77315.
- 20 F. Ni, Z. Wu, Z. Zhu, T. Chen, K. Wu, C. Zheng, K. An, D. Wei, D. Ma and C. Yang, *J. Mater. Chem. C*, 2017, **5**, 1363–1368.

